Slater Ice Rules and H-Bond Dynamics in KDP-Type Systems

Raymond Kind, Paola Maria Cereghetti, and Christian Anton Jeitziner
Institut für Quantenelektronik, Eidgenössiche Technische Hochschule Zürich-Hönggerberg, CH8093 Zürich, Switzerland

Boštjan Zalar, Janez Dolinšek, and Robert Blinc
J. Stefan Institute, University of Ljubljana, Jamova 39 1000 Ljubljana, Slovenia

(Received 16 January 2002; published 29 April 2002)

We report on the first observation of the dynamics of correlated hydrogen switching among the six Slater D_2PO_4 configurations, induced by unpaired D_3PO_4 and DPO_4 Takagi group diffusion in a deuteron glass $Rb_{0.5}(ND_4)_{0.5}D_2PO_4$. The results obtained by two-dimensional (2D) ^{31}P exchange NMR prove the validity of the Slater-Takagi ice rules and allow for the direct determination of the correlation time for the unpaired Takagi group visits to a given D_2PO_4 group.

DOI: 10.1103/PhysRevLett.88.195501 PACS numbers: 61.43.Fs, 64.70.Pf

Since the pioneering work of Slater in 1941 on the ferroelectric transition in KH_2PO_4 (KDP) [1] it is known that due to the so-called Pauling ice rules [2,3] only two out of the four protons linking adjacent PO_4 groups via double minimum type O-H$\cdots$O bonds are close to each PO_4 ion. A whole variety of such "Slater" lattices can be built with Slater H_2PO_4 groups, leading to a macroscopic degeneracy of possible ground states. There are six possible H_2PO_4 orientations, called the Slater configurations, with differently oriented electric dipole moments in KDP-type systems [1]. The two ferroelectric (FE) Slater configurations $FE_\uparrow$ and $FE_\downarrow$, with dipole moments along $+c$ and $-c$ axis, respectively, of the tetragonal crystal axes coordinate system $\overline{abc}$, are realized in the two 180° domains of the FE phase of KDP, whereas the four antiferroelectric (AFE) configurations $AFEa_\uparrow$, $AFEa_\downarrow$, $AFEb_\uparrow$, and $AFEb_\downarrow$, with respective dipole moments along $+a$, $-a$, $+b$, and $-b$, are found in the four 90° domains of the AFE phase of $NH_4H_2PO_4$ (ADP). In mixed KDP-ADP-type systems, there are randomly competing FE and AFE interactions as well as random fields, accompanied by frustration in the manifold of the Slater lattices. This prevents the system from becoming long-range ordered and leads into a disordered state with glasslike static and dynamic properties at low temperatures. It can be compared to the situation in hexagonal ice [2–4] where the H_2O molecules are frozen more or less randomly in one of the six possible orientations with equal probability.

In any Slater lattice, the double-well potential of a proton in an individual O−H$\cdots$O bond is asymmetric. This is so since any intrabond proton transfer from one well to another creates a Takagi [5] pair HPO_4–H_3PO_4 which has a higher energy than the Slater pair H_2PO_4–H_2PO_4 it is originating from. In contrast to that, an H bond linking an unpaired Takagi defect with a Slater group has a symmetric double well potential (Fig. 1). The dynamics of hydrogen bonds, or equivalently, the switching of Slater configurations, should therefore be driven by two processes: the creation-annihilation of Takagi pairs and the diffusion of unpaired Takagi defects over the lattice. The latter should take place with a much smaller activation energy than the former due to its nearly symmetric O–H$\cdots$O double minimum potential. The visits of Takagi groups to a given Slater group invert the bias of the H bonds (Fig. 1) in a stochastic way, thus symmetrizing the double well H-bond potential on the time average. So far the motion of unpaired Takagi groups was only postulated but no direct evidence in support of this mechanism has been found experimentally.

Here we report on the first determination of the mean correlation time between successive visits of unpaired Takagi groups to a given Slater group. The results were obtained by two-dimensional (2D) ^{31}P exchange NMR spectroscopy applied to a deuteron glass. We as well report on the observation of the correlated hydrogen switching dynamics among the six Slater H_2PO_4 configurations and

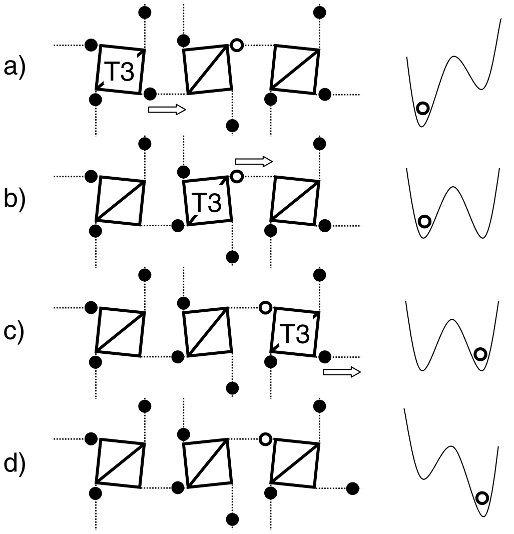

FIG. 1. Schematic illustration of the bond bias inversion in a random Slater lattice by the passage of an unpaired Takagi defect H_3PO_4 (T3). The left side shows configuration evolutions in four steps (a)–(d). Corresponding double well potentials of the deuteron (indicated by the open circle) are shown on the right side.

the direct measurement of the deuteron glass order parameter matrix on two different time scales: the 1D NMR time scale of $\simeq 10^{-4}$ s and the 2D NMR time scale of $\simeq 10$ s. Whereas the Edwards-Anderson glass order parameter is nonzero on the 1D NMR time scale, the local symmetry, broken at the glass transition, is restored on the 2D NMR time scale due to visits of unpaired Takagi groups.

Let us assume that we deal with a Slater lattice with a negligibly low concentration of Takagi defects. Although scarce, their dynamics (creation-annihilation or diffusion) provides for the Slater configurations' switching mechanism (Fig. 1). We shall describe the instantaneous orientational state of a given H_2PO_4 group as a six-component vector $\mathbf{w}_i = \{\delta_{ji}\}$ where the indices $i, j = \mathrm{FE}_\uparrow$, $\mathrm{FE}_\downarrow$, $\mathrm{AFE}a_\uparrow$, $\mathrm{AFE}a_\downarrow$, $\mathrm{AFE}b_\uparrow$, and $\mathrm{AFE}b_\downarrow$ denote the six Slater configurations. In the course of time, the initial "pure" state $\mathbf{w}_i$ develops into a mixed state

$$\mathbf{w}(t;i) = \exp(\mathcal{K}t)\mathbf{w}_i\,. \tag{1}$$

$\mathcal{K}$ is the 6×6 "exchange" matrix composed of probabilities per unit time for the transitions among the six Slater configurations. The jth component of $\mathbf{w}(t;i)$ can be regarded as a probability to find a given H_2PO_4 group in a state j at a time t provided its state was i at $t = 0$. The time average $\mathbf{w} = \overline{\mathbf{w}(t;i)}$, or equivalently, the thermodynamic average, is independent of the initial state i, $\mathbf{w} \neq f(i)$. $\mathbf{w}$ is time independent and corresponds to the stationary solution of Eq. (1), $d\mathbf{w}/dt = \mathcal{K}\mathbf{w} = 0$. The respective components w_j correspond to thermodynamically averaged local probabilities for the six Slater configurations $j = \mathrm{FE}_\uparrow$, $\mathrm{FE}_\downarrow$, $\mathrm{AFE}a_\uparrow$, $\mathrm{AFE}a_\downarrow$, $\mathrm{AFE}b_\uparrow$, and $\mathrm{AFE}b_\downarrow$. They are normalized ($\sum_j w_j = 1$) and can be combined into a symmetry-adapted five-component local order parameter vector $\boldsymbol{\psi} = (\mathbf{p}, p_\sigma, p_\eta)$, consisting of the local polarization vector $\mathbf{p} = (p_a, p_b, p_c) = (w_{\mathrm{AFE}a_\uparrow} - w_{\mathrm{AFE}a_\downarrow}, w_{\mathrm{AFE}b_\uparrow} - w_{\mathrm{AFE}b_\downarrow}, w_{\mathrm{FE}_\uparrow} - w_{\mathrm{FE}_\downarrow})$, the FE/AFE bias $p_\sigma = w_{\mathrm{FE}} - w_{\mathrm{AFE}}/2$, and the AFEa/AFEb bias $p_\eta = w_{\mathrm{AFEa}} - w_{\mathrm{AFEb}}$ local order parameters. Here $w_{\mathrm{FE}} = w_{\mathrm{FE}_\uparrow} + w_{\mathrm{FE}_\downarrow}$, $w_{\mathrm{AFEa}} = w_{\mathrm{AFE}a_\uparrow} + w_{\mathrm{AFE}a_\downarrow}$, $w_{\mathrm{AFEb}} = w_{\mathrm{AFE}b_\uparrow} + w_{\mathrm{AFE}b_\downarrow}$, and $w_{\mathrm{AFE}} = w_{\mathrm{AFEa}} + w_{\mathrm{AFEb}}$.

In a disordered system, the nonuniformness of the local order parameter $\boldsymbol{\psi}$ is taken into account by introducing the local order parameter distribution function $\mathcal{W}(\boldsymbol{\psi}) = \sum_{n=1}^{N} \delta(\boldsymbol{\psi} - \boldsymbol{\psi}_n)$ in analogy to the local magnetization distribution function in spin glasses [6]. N is the number of PO_4 sites. The first moment of $\mathcal{W}(\boldsymbol{\psi})$ corresponds to the long-range order parameter vector $\boldsymbol{\Psi} = \langle \boldsymbol{\psi} \rangle = (\mathbf{P}, P_\sigma, P_\eta)$ where $\langle \cdots \rangle$ stands for the averaging over $\mathcal{W}(\boldsymbol{\psi})$, i.e., $\langle f(\boldsymbol{\psi}) \rangle = \int f(\boldsymbol{\psi}) \mathcal{W}(\boldsymbol{\psi})\, d^5\psi$. In $\mathbf{P} = (P_a, P_b, P_c) = (\langle p_a \rangle, \langle p_b \rangle, \langle p_c \rangle) = \langle \mathbf{p} \rangle$ we recognize the macroscopic polarization, while $P_\sigma = \langle p_\sigma \rangle$ and $P_\eta = \langle p_\eta \rangle$ are parameters measuring the prevalence of FE ordering over AFE ordering and the prevalence of AFEa ordering over AFEb ordering, respectively. The long-range order parameter of a Slater lattice thus consists of five components $P_k \in [-1, 1]$, $k = a, b, c, \sigma, \eta$.

The disorder is reflected in a nonzero value of the matrix $\mathcal{Q} = \langle (\boldsymbol{\psi} - \boldsymbol{\Psi}) \otimes (\boldsymbol{\psi} - \boldsymbol{\Psi}) \rangle$, which we recognize as a generalized glass order parameter tensor with components $Q_{kl} = \langle p_k p_l \rangle - P_k P_l$. There are, in general, 15 independent components, since $\mathcal{Q}$ is a symmetric tensor. It is straightforward to show that the sum of the first three diagonal elements, $Q_{aa} + Q_{bb} + Q_{cc}$, is equivalent to the well-known Edwards-Anderson glass order parameter $q_{\mathrm{EA}} = \langle p^2 \rangle - P^2$ [6].

If one disregards higher moments of $\mathcal{W}(\boldsymbol{\psi})$, the set $\{\boldsymbol{\psi}, \mathcal{Q}\}$ of 20 parameters completely describes the thermodynamic state of any ordered/disordered Slater lattice. We shall now show that all these parameters, as well as the Slater configuration's switching dynamics time scale, can be measured by ^{31}P 2D exchange NMR.

Our experimental method is based on the fact that ^{31}P chemical shift tensors discriminate among different H_2PO_4 Slater configurations. At low temperature, ^{31}P 1D NMR probes the instantaneous configurations of H_2PO_4 groups [7]. In a simplified picture, at a general orientation of the crystal, there are six absorption peaks with frequencies corresponding to the six Slater configurations i. Their respective normalized NMR absorption intensities $I_i = I(\omega_i)$ are equivalent to the disorder-averaged probabilities w_i, $I_i = \langle w_i \rangle$. The 1D spectral peak intensities can be represented in the vector form as $\mathbf{I}_{\mathrm{1D}} = \{\langle w_i \rangle\} = f(\boldsymbol{\Psi})$. Measurements of $\mathbf{I}_{\mathrm{1D}}$ thus yield the long-range order parameter $\boldsymbol{\Psi}$. In contrast to the fast motion regime realized at high temperatures where the glass order parameter $\mathcal{Q}$ can be obtained from the 1D spectral shapes [8], no information about the glass order parameter can be obtained from the 1D ^{31}P NMR spectra in the slow motion regime at low temperatures [9]. Such information can, however, be extracted from the 2D exchange NMR experiment in which two states i and j at times $t = 0$ and $t = \tau_{\mathrm{mix}}$ are correlated. When no exchange between i and j takes place during the mixing period τ_{mix}, the absorption peaks corresponding to these two states lie on the diagonal of the 2D ω_1 vs ω_2 spectrum at (ω_i, ω_i) and (ω_j, ω_j). If exchange does take place, we obtain in addition to the diagonal peaks also cross peaks at (ω_i, ω_j) and (ω_j, ω_i) [10]. Their intensities depend on τ_{mix}. The corresponding 2D matrix of spectral peak intensities can be written as $\mathcal{I}_{\mathrm{2D}}(\tau_{\mathrm{mix}}) = \{\langle w_j(\tau_{\mathrm{mix}}; i) w_i \rangle\}$ and is normalized for any τ_{mix}, $\sum_{i,j} \langle w_j(\tau_{\mathrm{mix}}; i) w_i \rangle = 1$. At zero mixing time this matrix is diagonal and thus equivalent to the 1D spectrum: $\mathcal{I}_{\mathrm{2D}}(0) = \{\delta_{ji} \langle w_i \rangle\} = f(\boldsymbol{\Psi})$. In the $\tau_{\mathrm{mix}} \to \infty$ limit, on the other hand, there is no correlation between the initial state i and the final state j; this results in $\mathcal{I}_{\mathrm{2D}}(\infty) = \{\langle w_j w_i \rangle\} = f(\boldsymbol{\Psi}, \mathcal{Q})$. The above 2D exchange matrix contains 20 independent elements. This makes it possible to determine independently the 20 order parameter components $\{\boldsymbol{\Psi}, \mathcal{Q}\}$ describing the Slater lattices.

In a disordered Slater lattice, there is no long-range polar order, i.e., $P_a = P_b = P_c = 0$. The results described in [9] also reveal vanishing polar glass order on the 2D deuteron exchange NMR time scale, i.e., $Q_{aa} = Q_{bb} = Q_{cc} = 0 \Rightarrow q_{\mathrm{EA}} = 0$. As demonstrated above, the remaining order parameters can be determined via ^{31}P 2D exchange NMR. The FE/AFE bias long-range order parameter P_σ and the glass order parameter $Q_{\sigma\sigma} = \langle p_\sigma^2 \rangle - P_\sigma^2$, never measured before in a disordered KDP-type system, are here of a major interest.

The deuteron glass [8,9,11–13] we investigated is a $\mathrm{Rb}_{0.5}(\mathrm{ND}_4)_{0.5}\mathrm{D}_2\mathrm{PO}_4$ (DRADP-50) single crystal, i.e., a solid solution of ferroelectric $\mathrm{RbD}_2\mathrm{PO}_4$ and antiferroelectric $\mathrm{ND}_4\mathrm{D}_2\mathrm{PO}_4$. Below $T \simeq 60$ K, ^{31}P 2D exchange NMR probes the instantaneous Slater orientations of $\mathrm{D}_2\mathrm{PO}_4$ groups (Fig. 2a). No separate lines corresponding to Takagi groups have been observed demonstrating that the concentration of the Takagi groups is much lower than the concentration of the Slater groups.

There exists a special orientation $\mathbf{B}_0 \perp \mathbf{c}, \theta\angle(\mathbf{B}_0, \mathbf{a}) = 45°$, where all four antiferroelectric $\mathrm{H}_2\mathrm{PO}_4$ configurations are equivalent (Fig. 2b). In this case, the ^{31}P 2D exchange NMR peak intensity matrix reduces to a 3 × 3 matrix $\mathcal{I}_{2D}(\tau_{\mathrm{mix}}) = \{I_{ji}(\tau_{\mathrm{mix}})\}$; $i, j = \mathrm{FE}_\uparrow, \mathrm{FE}_\downarrow, \mathrm{AFE}$. It is diagonal at zero mixing time. Its respective elements can be written in terms of the long range order parameters P_c and P_σ:

$$I_{\mathrm{FE}_\uparrow\text{-}\mathrm{FE}_\uparrow} = 1/2P_c + 1/3P_\sigma + 1/6, \tag{2a}$$

$$I_{\mathrm{FE}_\downarrow\text{-}\mathrm{FE}_\downarrow} = -1/2P_c + 1/3P_\sigma + 1/6, \tag{2b}$$

$$I_{\mathrm{AFE}\text{-}\mathrm{AFE}} = 2/3(1 - P_\sigma). \tag{2c}$$

In the $\tau_{\mathrm{mix}} \to \infty$ limit, the $I_{\mathrm{AFE}\text{-}\mathrm{FE}_\uparrow}$, $I_{\mathrm{FE}_\uparrow\text{-}\mathrm{AFE}}$, $I_{\mathrm{FE}_\downarrow\text{-}\mathrm{FE}_\uparrow}$, $I_{\mathrm{FE}_\uparrow\text{-}\mathrm{FE}_\downarrow}$, $I_{\mathrm{FE}_\downarrow\text{-}\mathrm{AFE}}$, and $I_{\mathrm{AFE}\text{-}\mathrm{FE}_\downarrow}$ cross peaks are also present. The 2D exchange matrix elements are here related to the order parameter components via

$$\begin{aligned} I_{\mathrm{FE}_\uparrow\text{-}\mathrm{FE}_\uparrow} = {} & 1/4(Q_{cc} + P_c^2) + 1/9(Q_{\sigma\sigma} + P_\sigma^2 + P_\sigma) \\ & + 1/3(Q_{c\sigma} + P_c P_\sigma) + 1/6P_c + 1/36, \end{aligned} \tag{3a}$$

$$I_{\mathrm{AFE}\text{-}\mathrm{AFE}} = 4/9(Q_{\sigma\sigma} + P_\sigma^2 - 2P_\sigma) + 4/9, \tag{3b}$$

$$\begin{aligned} I_{\mathrm{FE}_\downarrow\text{-}\mathrm{FE}_\downarrow} = {} & 1/4(Q_{cc} + P_c^2) + 1/9(Q_{\sigma\sigma} + P_\sigma^2 + P_\sigma) \\ & - 1/3(Q_{c\sigma} + P_c P_\sigma) - 1/6P_c + 1/36, \end{aligned} \tag{3c}$$

$$\begin{aligned} I_{\mathrm{AFE}\text{-}\mathrm{FE}_\uparrow} = I_{\mathrm{FE}_\uparrow\text{-}\mathrm{AFE}} = {} & 1/3P_c - 1/3(Q_{c\sigma} + P_c P_\sigma) \\ & + 1/9(P_\sigma - 2Q_{\sigma\sigma} - 2P_\sigma^2) + 1/9, \end{aligned} \tag{3d}$$

$$\begin{aligned} I_{\mathrm{FE}_\downarrow\text{-}\mathrm{FE}_\uparrow} = I_{\mathrm{FE}_\uparrow\text{-}\mathrm{FE}_\downarrow} = {} & -1/4(Q_{cc} + P_c^2) \\ & + 1/9(Q_{\sigma\sigma} + P_\sigma^2 + P_\sigma) + 1/36, \end{aligned} \tag{3e}$$

$$\begin{aligned} I_{\mathrm{FE}_\downarrow\text{-}\mathrm{AFE}} = I_{\mathrm{AFE}\text{-}\mathrm{FE}_\downarrow} = {} & -1/3P_c + 1/3(Q_{c\sigma} + P_c P_\sigma) \\ & + 1/9(P_\sigma - 2Q_{\sigma\sigma} - 2P_\sigma^2) + 1/9. \end{aligned} \tag{3f}$$

Measurements of the normalized 2D exchange peak intensities thus allow for the determination of all five order parameter components P_c, P_σ, Q_{cc}, $Q_{\sigma\sigma}$, and $Q_{c\sigma}$. The experimentally observed ^{31}P 2D exchange NMR spectrum of DRADP-50 at 55 K taken with a mixing time of 800 ms is compared with the theoretical ^{31}P 2D exchange NMR spectrum in Fig. 3. The observed spectrum consists of a strong AFE diagonal peak and two weaker $\mathrm{FE}_\uparrow$ and $\mathrm{FE}_\downarrow$ diagonal peaks as well as of AFE ↔ $\mathrm{FE}_\uparrow$ and AFE ↔ $\mathrm{FE}_\downarrow$ cross peaks. The rather weak $\mathrm{FE}_\downarrow$ ↔ $\mathrm{FE}_\uparrow$ cross peaks are present as well. The agreement between the observed and theoretical 2D exchange spectrum is excellent and directly

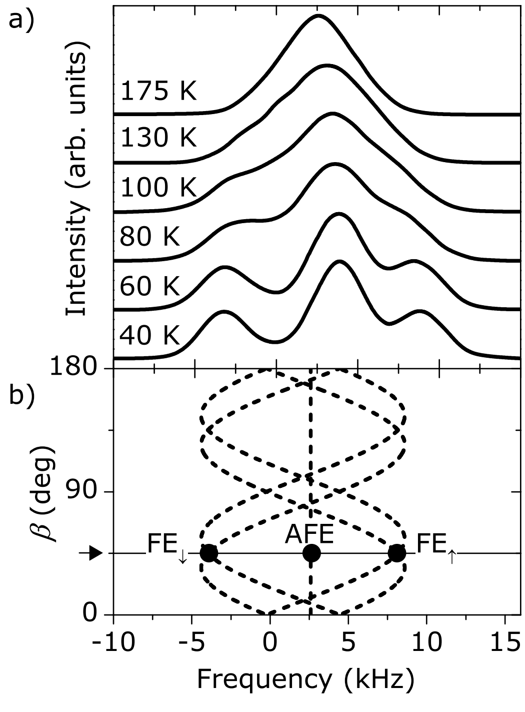

FIG. 2. (a) ^{31}P NMR spectra as a function of temperature for the crystal orientation $\mathbf{B}_0 \perp \mathbf{c}, \theta\angle(\mathbf{B}_0, \mathbf{a}) = 45°$. The observed increase of the inhomogeneous line shape broadening with decreasing temperature reflects the onset of the static glass disorder on the 1D ^{31}P NMR time scale. The Edwards-Anderson order parameter at $T = 60$ K amounts to $q_{\mathrm{EA}} \simeq 0.6$. Below this temperature, well-resolved absorption peaks corresponding to different Slater $\mathrm{D}_2\mathrm{PO}_4$ configurations are seen. (b) Calculated ^{31}P low temperature rotation pattern for $\mathbf{B}_0$ rotating in the $\overline{ab}$ plane of the crystal. The orientation at which the 1D and 2D spectra were taken is indicated by an arrow.

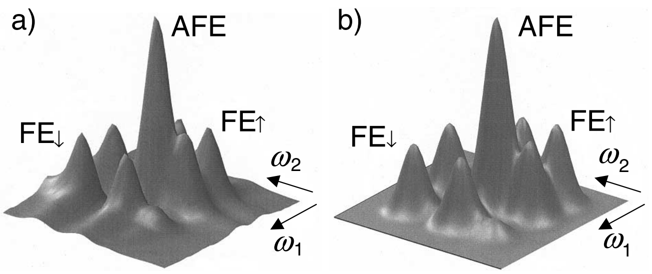

FIG. 3. Experimental (a) and theoretical (b) 2D ^{31}P exchange NMR spectra of DRADP-50. The spectra were taken at $\mathbf{B}_0 \perp \mathbf{c}, \theta\angle(\mathbf{B}_0, \mathbf{a}) = 45°$, and $T = 55$ K with a mixing time of 800 ms.

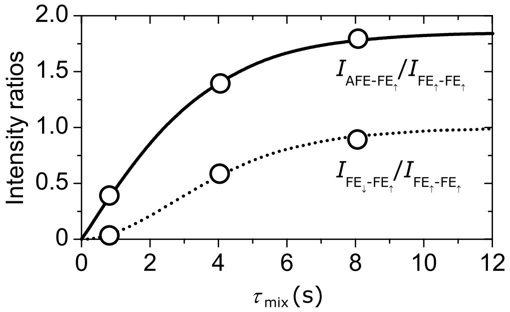

FIG. 4. Ratio of the integrated intensities of the AFE-FE$_\uparrow$ and FE$_\downarrow$-FE$_\uparrow$ cross peaks to the diagonal peak FE$_\uparrow$-FE$_\uparrow$ in DRADP-50 as a function of the mixing time at $T = 45$ K. The solid and dotted lines represent theoretical fits to Eq. (1) yielding $\tau_{\text{exch}} \simeq 15$ s.

proves the occurrence of transitions between the AFE and FE configurations and vice versa.

At $T = 45$ K, the experimental 2D ^{31}P data for $\tau_{\text{mix}} = 0$ yield $P_c = 0$, $P_\sigma = 0.27$ whereas the data for $\tau_{\text{mix}} \to \infty$ yield $P_c = 0$, $P_\sigma = 0.27$, $Q_{cc} = 0$, $Q_{\sigma\sigma} = 0$, and $Q_{c\sigma} = 0$. The same P_c and P_σ values are obtained in both cases, supporting the validity of our model.

$P_c = 0$ and $Q_{cc} = 0$ demonstrate that both polar long-range and polar glass order parameters vanish on the 2D NMR time scale, also confirming the deuteron 2D exchange NMR results [9]. The $P_\sigma = \langle w_{\text{FE}} - w_{\text{AFE}}/2 \rangle = 0.27$ result shows that the FE Slater configurations are here more probable on the time average than the AFE ones. The vanishing FE/AFE glass order parameter $Q_{\sigma\sigma} = \langle p_\sigma^2 \rangle - P_\sigma^2 = 0$ reveals that all locally inhomogeneous FE/AFE bias fluctuations, in addition to polar fluctuations, are averaged out due to Takagi group visits. This motion inverts the bias of the D bonds of the Slater D_2PO_4 groups in a stochastic way (Fig. 1) and thus symmetrizes the $\text{O-D} \cdots \text{O}$ bonds on the time average. The local surrounding of all PO_4 groups is identical on the time scale of the 2D experiment, yielding $q_{\text{EA}} = 0$, whereas it differs on the much shorter 1D NMR time scale, resulting in a nonzero q_{EA} (Fig. 2a).

The time scale of the exchange among different Slater configurations is obtained by fitting the measured $I_{\text{2D}}(\tau_{\text{mix}})$ to Eq. (1) with $t = \tau_{\text{mix}}$. The results for $T = 45$ K are shown in Fig. 4. Both the AFE-FE$_\uparrow$/FE$_\uparrow$-FE$_\uparrow$ and FE$_\downarrow$-FE$_\uparrow$/FE$_\uparrow$-FE$_\uparrow$ cross to diagonal peak intensity ratios approach the saturation ($\tau_{\text{mix}} \to \infty$) values 1.89 and 1, respectively, with a characteristic time $\tau_{\text{exch}} \simeq 15$ s. The above saturation values directly reflect the measured values of the order parameter components using Eqs. (3). Solutions of Eq. (1) with a 3×3 exchange matrix $\mathcal{K}$ in general involve two-exponential behavior. τ_{exch} is therefore an effective time scale of the successive visits of unpaired Takagi groups to a given Slater group. This parameter has never before been measured in any KDP-type ordered/disordered system. In our specific case it is evidently much longer than the correlation times deduced from the Rb and deuteron spin-lattice relaxation time data at high temperatures [14–16] which yield for the intra-D-bond deuteron jump time $\tau = 10^{-11}$–10^{-12} s.

We have thus directly proved the exchange between FE and AFE Slater configurations in DRADP. As known since the early work of Slater and Takagi, this exchange can take place at low temperatures exclusively via diffusion of unpaired Takagi groups. These groups, once created, move around for long distances with little or no activation energy in a nearly symmetric H-bond potential and rearrange many Slater groups before recombination. At higher temperatures, on the other hand, the concentration of Takagi groups is high and their mean free path short. The frustrated H-bond dynamics and the Rb and deuteron spin-lattice relaxation processes are here not governed by unpaired Takagi group diffusion but by Takagi group creation and annihilation, requiring a much higher activation energy.

The above results thus represent the first direct measurement of the time scale for successive visits of unpaired Takagi groups to a given Slater group. They also confirm the validity of the Slater ice rules as introduced by Pauling [3], Slater [1], and Takagi [5] in the 1940s and 1950s and at the same time explain the symmetry properties of these systems [17] which are in apparent contradiction with the above rules.

[1] J. C. Slater, J. Chem. Phys. **9**, 16 (1941).
[2] J. D. Bernal and R. H. Fowler, J. Chem. Phys. **1**, 515 (1933).
[3] L. Pauling, in *The Nature of the Chemical Bond* (Cornell University Press, Ithaca, New York, 1945).
[4] A. P. Ramirez, A. Hayashi, R. J. Cava, R. Siddharthan, and B. S. Shastry, Nature (London) **399**, 333 (1999).
[5] Y. Takagi, J. Phys. Soc. Jpn. **3**, 273 (1948).
[6] S. F. Edwards and P. W. Anderson, J. Phys. F **5**, 965 (1975); see also K. Binder and A. P. Young, Rev. Mod. Phys. **58**, 801 (1986).
[7] R. Blinc, M. Burgar, V. Rutar, J. Seliger, and I. Zupančič, Phys. Rev. Lett. **38**, 92 (1977).
[8] R. Blinc, J. Dolinšek, R. Pirc, B. Tadić, B. Zalar, R. Kind, and O. Liechti, Phys. Rev. Lett. **63**, 2248 (1989).
[9] J. Dolinšek, B. Zalar, and R. Blinc, Phys. Rev. B **50**, 805 (1994); J. Dolinšek, B. Zalar, and R. Blinc, Z. Naturforsch. A **49**, 329 (1994).
[10] C. Schmidt, R. Blumich, and H. W. Spiess, J. Magn. Reson. **79**, 269 (1988).
[11] N. Korner and R. Kind, Phys. Rev. B **49**, 5918 (1994); R. Kind, N. Korner, T. Koenig, and C. Jeitziner, J. Korean Phys. Soc. **32**, S799 (1998).
[12] V. H. Schmidt, J. Korean Phys. Soc. **32**, S803 (1998).
[13] R. Pirc, B. Tadić, and R. Blinc, Phys. Rev. B **36**, 8607 (1987).
[14] J. Dolinšek, D. Arčon, B. Zalar, R. Pirc, R. Blinc, and R. Kind, Phys. Rev. B **54**, R6811 (1996).
[15] N. Korner, C. Pfammatter, and R. Kind, Phys. Rev. Lett. **70**, 1283 (1993).
[16] V. H. Schmidt and E. A. Uehling, Phys. Rev. **126**, 447 (1962).
[17] J. L. Bjorkstam, Phys. Rev. **153**, 599 (1967).